Available online at www.sciencedirect.com
SCIENCE DIRECT®
Applied Thermal Engineering 25 (2005) 783–795
APPLIED THERMAL ENGINEERING
www.elsevier.com/locate/apthermeng

The influence of the space between the billets on the productivity of a continuous walking-beam furnace

Anton Jaklič [a,*], Tomaž Kolenko [b], Borut Zupančič [c]

[a] *Institute of Metals and Technology, Lepi pot 11, 1000 Ljubljana, Slovenia*
[b] *Faculty of Natural Science and Technology, University of Ljubljana, Aškerčeva 12, 1000 Ljubljana, Slovenia*
[c] *Faculty of Electrical Engineering, University of Ljubljana, Tržaška 25, 1000 Ljubljana, Slovenia*

Received 13 January 2004; accepted 24 July 2004
Available online 25 September 2004

Abstract

This paper presents a study of the influence of the space between billets on the productivity of a continuous walking-beam furnace. The study was performed using a simulation model of a billet-reheating process for three different billet dimensions. The simulation model considered the exact geometry of the furnace enclosure, including the geometry of the billets inside the furnace. A view-factor matrix of the furnace enclosure was determined using the Monte Carlo method. The heat exchange between the furnace gas, the furnace wall and the billet's surface was calculated using a three-temperature model. The temperature of the furnace floor was determined using a heat-balance equation, and the heat conduction in the billets was calculated using the 3D finite-difference method. The model was validated using measurements from trailing thermocouples positioned in the test billet during the reheating process in the furnace.

Keywords: Steel industry; Simulation model; Billet heating; Furnace; Productivity

* Corresponding author. Tel.: +386 1 4701 999; fax: +386 1 4701 939.
E-mail address: anton.jaklic@imt.si (A. Jaklič).

1359-4311/$ - see front matter
doi:10.1016/j.applthermaleng.2004.07.012

Nomenclature

a	heat-transfer coefficient ($\mathrm{W\,m^{-2}\,K^{-1}}$)
a	vector for the description of a general rectangular surface
A	surface area ($\mathrm{m^2}$)
b	vector for the description of a general rectangular surface
d	furnace-wall/floor-layer thickness (m)
e	vector of photon emission
F	view-factor
F	view-factor matrix
I	number of surfaces in a furnace enclosure
K	number of the furnace-wall/floor-layers
L	length (m)
M	number of the furnace-floor surfaces
N	number of photons
q	heat flux ($\mathrm{W\,m^{-2}}$)
R	random number
T	temperature (K)
x	vector from the coordinate base to the point on the surface
X	point on the surface

Greek letters

α	absorptivity factor
ε	emissivity factor
ϕ	angle in spherical coordinate system (rad)
ϕ	diameter (mm)
λ	heat conduction ($\mathrm{W\,m^{-1}\,K^{-1}}$)
π	number PI
σ	Stefan–Boltzmann constant, $\sigma = 5.671 \times 10^{-8}\ \mathrm{W\,m^{-2}\,K^{-4}}$
θ	angle in spherical coordinate system (rad)

Subscripts

abs	absorption
air	air
b	billet
cond	conduction
E	emission
floor	furnace floor
g	furnace gas
w	furnace wall
i	index of surface in furnace enclosure
j	index of surface in furnace enclosure

k	index of layers of furnace wall/floor
m	index of furnace-floor surface
n	index of furnace-floor surface
rad	radiation
$\rightarrow$	outgoing
$\leftarrow$	incoming

1. Introduction

Optimising energy-intensive processes plays an important role in the steel industry's drive to introduce cleaner and more efficient forms of production. Industrial furnaces are usually the critical pieces of equipment in the industrial production chain, for the following reasons: they consume a large amount of energy, they have an important influence on the quality of the final product, they account for a large proportion of the production time and they have a major impact on the levels of pollution that are generated by the plant [1].

The hot-rolling process for steel billets requires high-quality reheated billets. And these billets are often reheated in a gas-fired, continuous walking-beam furnace (Fig. 1).

In a walking beam furnace, the billets are transported through the furnace by the action of the so-called walking beam. The complete walking-beam step consists of the following segments: raising the beam with all the billets, shifting the beam with the billets over a length of one step, lowering the beam to put the billets on the floor, shifting the beam back to the start position, discharging the billet at the last position from the furnace and charging a new billet to the first position in the furnace. The length of the beam step can, however, be varied.

In an earlier publication, we reported on a new transport system for moving the billets from the reheating furnace to a rolling mill [4]. The system allows one furnace to serve two rolling mills. During the production process we observed that the productivity of the rolling mills is greater than that of the furnace. As a result, we decided to look into the possibility of increasing the furnace's productivity in order to increase the overall production capabilities. One possibility that we identified was to alter the space between the billets.

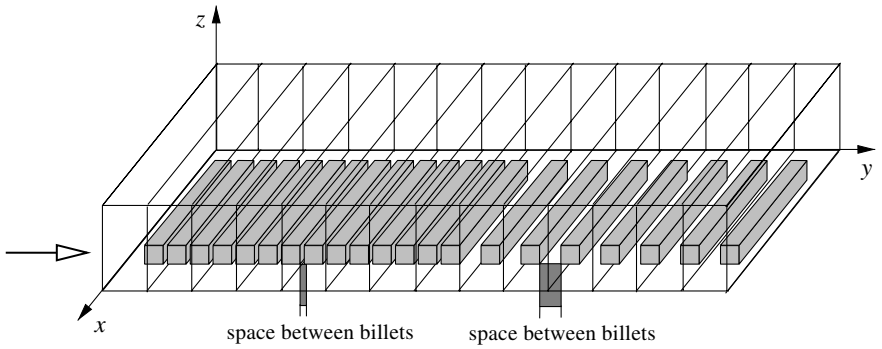

Fig. 1. A walking-beam furnace.

The productivity of a continuous, walking-beam furnace is defined as the weight of reheated billets per unit time. In this case, reheated means that the billets are reheated to the prescribed final temperature in the middle of the billet with an acceptable temperature difference between the upper and lower surfaces of the billet. For billets that are of the same size and the same grade of steel, the productivity is directly related to the frequency of discharged billets (the beam steps). Reheating conditions are, however, different for different spaces between billets at the same step frequency. In the case of small spaces between billets (short beam steps) the reheating time in the furnace is long: the billets are close to each other; the reheating is asymmetrical, mostly through the upper surface of the billet; and the furnace floor is colder because it is mainly reheated indirectly through the billets. In the case of long spaces between billets (long beam steps) the reheating time is short: the distance between the billets allows more symmetrical reheating; the furnace floor is warmer because it is mostly reheated directly from the furnace walls and the furnace gas. This suggests that there is an optimum space between the billets, where the highest productivity lies.

Based on practical experiences, Schuppe [8] suggests a wide interval for the highest productivity. However, for optimising a particular furnace, the dependence of the productivity on the space between the billets is required. One possible way to obtain this dependence is to use a simulation model, which allows us to experiment with a wide range of spaces and with billets of different sizes.

In order to optimise the billet-reheating process in a walking-beam furnace we developed a simulation model. The model is based on the main physical phenomena of the reheating process in a natural-gas-fired walking-beam furnace: thermal radiation is the main heat-transfer mechanism, and the geometry of the furnace enclosure has an important role in the heat transfer of the thermal radiation. The furnace enclosure consists of the furnace geometry together with the geometry of the charged billets inside the furnace. This means that the geometry of the continuous furnace enclosure becomes very complex when there are hundreds of billets in the furnace and reflected radiation becomes a factor. When experimenting with the space between the billets and with the size of the billets, the geometry of the furnace enclosure will change. So in order to study the productivity dependencies, the geometry of the furnace enclosure has to be treated very accurately in the model.

One of the chief mathematical complexities in treating radiative heat transfer between surfaces is accounting for the geometrical relations involved in how the surfaces view each other. For the whole furnace enclosure, they are expressed with a view-factor matrix form. In order to determine the matrix, a separate simulation model based on the Monte Carlo method was developed. This model allows a view-factor determination for a general furnace enclosure consisting of rectangular surfaces. When the view-factor matrix for a particular furnace enclosure, including the billets, is known, it can be read into the simulation model of the billet-reheating process.

The aim of this study was to find out how the furnace productivity was affected by using different charging spaces between the billets for different billet dimensions. Once the productivity curves are known, it would be possible to find the optimum space between the billets that gives the highest furnace productivity for an individual billet size.

2. Determination of the view-factor matrix using the Monte Carlo method

The calculation of the thermal radiation heat transfer between two surfaces can be divided into the energy and the geometry parts [6]. The main part of the calculation of the thermal radiation

heat exchange between the surfaces in the furnace enclosure is the determination of a view-factor matrix **F**. The elements of the matrix are the view-factors $F_{i\to j}$ that describe the fraction of the total thermal radiation emitted by surface A_i that is absorbed by surface A_j, including multiple reflections. Since some of the surfaces in the enclosure cannot view each other and some can only be viewed partly, the furnace enclosure presents a complex geometry for the view-factor calculation.

Since energy travels in discrete photon bundles along a straight path before interacting with a surface [6], problems in thermal radiation are particularly well suited to the Monte Carlo method. In the case of determining view-factors, a large number N_i of photons are emitted from the surface, i.e., A_i. These photons are emitted from the surface according to probability density functions. The path of each photon, including possible reflections, is traced to its absorption at one of the surfaces of the furnace enclosure. In the model, the emission and the reflection of photons are treated as grey and diffuse. Thus, determining view-factors in the furnace enclosure with the Monte Carlo method implies emitting and tracing the history of a statistically meaningful random sample of photons from their points of emission to their points of absorption, including multiple reflections. After the emission of a large number of photons N_i from a surface A_i, the view-factor $F_{i\to j}$ can be directly determined by counting the number of photons $N_{i\to j}$ that have been absorbed at the surface A_j [6]:

$$F_{i\to j} = \lim_{N_i\to\infty}\left(\frac{N_{i\to j}}{N_i}\right) \approx \left(\frac{N_{i\to j}}{N_i}\right)_{N_i\gg 1} \tag{1}$$

The emission of an individual photon from surface A_i is determined by the point of emission X_{E} and by the direction of emission **e** (Fig. 2).

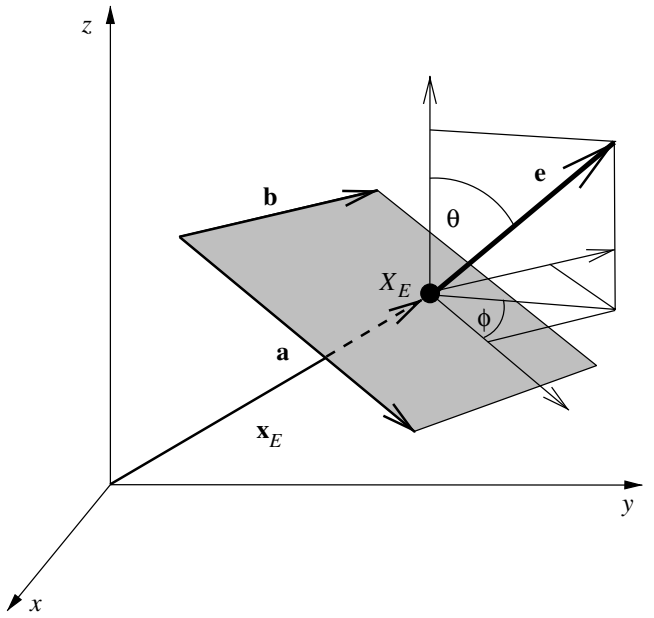

Fig. 2. Photon emission.

The random-number generator Mersenne–Twister [5], which is equally distributed in interval $[0, 1]$ was used in the model. The probability of emission from the rectangular surface A_i is equally distributed across the whole surface. The point of emission X_E can thus be determined by multiplying vectors **a** and **b** by two random numbers R_1 and R_2:

$$\mathbf{x}_E = R_1\mathbf{a} + R_2\mathbf{b} \tag{2}$$

The direction of emission is determined by the angles θ and ϕ. In the model, a grey diffuse emission and reflection approximation is assumed. In this case θ and ϕ can be determined using two random numbers R_3 and R_4 [2,7]:

$$\begin{aligned} \theta &= \sin^{-1}(\sqrt{R_3}) \\ \phi &= 2\pi R_4 \end{aligned} \tag{3}$$

The path of each photon is traced using a photon-tracing algorithm. The photon can interact on its path with one of the surfaces of observed geometry. When the photon-surface interaction occurs, a new random number R_i is generated. If $R_i \leqslant \varepsilon_k$, then it is assumed in the model that the photon is absorbed at surface A_k, else the reflection of the photon occurs. Reflections are treated using the point of interception as a point of reflection. The direction of diffuse reflection is treated using the same equations as used for the direction of emission.

3. The simulation model used for the billet reheating

3.1. Heat exchange in the furnace

Billets are reheated in a gas-fired continuous furnace. The heat-exchange phenomena between the furnace gas, the furnace wall and the billet surface is treated using basic algorithms of the modified three-temperature model of Heiligenstaedt [3]. The model is based on three temperatures: the furnace-gas temperature T_g, the furnace-wall temperature T_w and the billet-surface temperature T_b. All three temperatures have to be known for an evaluation of the temperature-dependent heat fluxes in the system. The modification of the model assumes that the furnace-wall temperature can be measured more reliably than the furnace-gas temperature. Therefore, the furnace-wall temperature was taken as the model's primary value; in contrast to the original model, where this was the furnace-gas temperature. The model was also improved to take into account the geometry of the furnace enclosure, including the billets. The model assumes that the furnace-gas temperature is homogenous, and so to comply with this assumption the length of the furnace is divided into smaller segments.

The heat exchange in the furnace segment is shown in Fig. 3(a). The furnace gas has the highest temperature T_g in the system and emits heat to the furnace wall ($q_{\mathrm{rad\,gw}}$, $q_{\mathrm{conv\,gw}}$) and to the billet surface ($q_{\mathrm{rad\,gb}}$, $q_{\mathrm{conv\,gb}}$) by radiation and convection. A fraction of the heat to the furnace wall is lost to the outside, through the furnace wall ($q_{\mathrm{cond\,w}}$), and another fraction is emitted to the billet surface ($q_{\mathrm{rad\,wb}}$), where it is partly absorbed by the furnace gas ($q_{\mathrm{abs\,g}}$). The inner furnace-wall temperature T_w is known; it can be measured with a thermocouple mounted in the furnace wall. The billet-surface temperature is also known; it is calculated step-by-step, using the finite difference

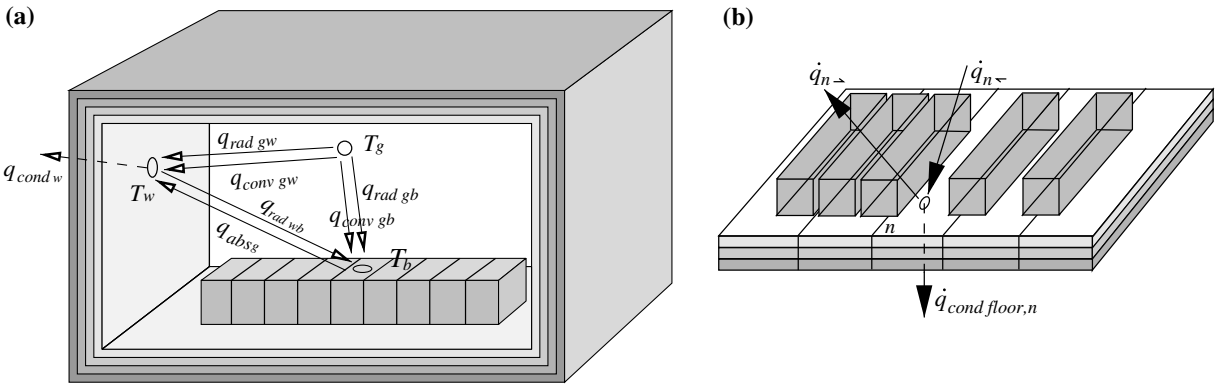

Fig. 3. (a) The heat exchange in the furnace segment, (b) the heat-flux balance for determining the temperature of the furnace floor.

method. The only unknown temperature in the system is the furnace-gas temperature T_g; this can be evaluated by solving an equilibrium equation on the inner furnace wall:

$$0 = q_{\mathrm{rad\,gw}}(T_g, T_w)A_w + q_{\mathrm{conv\,gw}}(T_g, T_w)A_w - q_{\mathrm{cond\,w}}(T_w)A_w - q_{\mathrm{rad\,wb}}(T_w, T_b)A_b + q_{\mathrm{abs\,g}}(T_w, T_b)A_b \quad (4)$$

In Eq. (4), A_w is the area of the wall surface of the furnace segment, A_b is the area of the billet surface that is surrounded by the furnace-wall segment. The above equation can be solved numerically using the bisection method. The $q_{\mathrm{rad\ gw}}(T_g, T_w)$ is calculated by Eq. (5); it describes the difference between the emitted heat flux from the gas mixture and the absorbed heat flux emitted from the furnace wall. The values for ε_g and α_g are determined using the model for a grey-gas CO_2 and H_2O mixture of Hottel [7].

$$q_{\mathrm{rad\,gw}}(T_g, T_w) = \varepsilon_g(T_g)\sigma T_g^4 - \alpha_g(T_g, T_w)\sigma T_w^4 \quad (5)$$

The $q_{\mathrm{conv\,gw}}(T_g, T_w)$ in (4) can be determined using Eq. (6). The convection heat transfer in a high-temperature reheating furnace has a minor influence on the reheating process, especially in the high-temperature part of the furnace. Different authors recommend different values for a_{gw} between 10 and 15 W/m^2K. In our model we used $a_{gw} = 12\,W/m^2K$.

$$q_{\mathrm{conv\,gw}}(T_g, T_w) = a_{gw} \cdot (T_g - T_w) \quad (6)$$

For the evaluation of the furnace-gas temperature T_g of the furnace segment (4) the average heat flux between the furnace wall and the billet surface $q_{\mathrm{rad\,wb}}(T_w, T_b)$ is determined by (7):

$$q_{\mathrm{rad\,wb}}(T_w, T_b) = \frac{\varepsilon_w(T_w)\sigma T_w^4 - \varepsilon_b(T_b)\sigma T_b^4}{\frac{1}{\varepsilon_b} + \frac{A_b}{A_w}\left(\frac{1}{\varepsilon_w} - 1\right)} \quad (7)$$

The part of the heat exchange between the furnace wall and the billet surface that is absorbed in the furnace gas $q_{\mathrm{abs\,g}}$ is determined by Eq. (8). It is determined as the radiation of the furnace gas to the billet surface, where the furnace gas is at the furnace-wall temperature [3]. The values for ε_g and α_g are determined using the model for a grey-gas CO_2 and H_2O mixture of Hottel [7].

$$q_{\mathrm{abs\,g}}(T_{\mathrm{w}}, T_{\mathrm{b}}) = \varepsilon_{\mathrm{g}}(T_{\mathrm{w}})\sigma T_{\mathrm{w}}^4 - \alpha_{\mathrm{g}}(T_{\mathrm{w}}, T_{\mathrm{b}})\sigma T_{\mathrm{b}}^4 \tag{8}$$

The heat conduction through a multi-layer (K) furnace wall $q_{\mathrm{cond\,w}}$ is calculated using Eq. (9). The thermal conductivities λ_k of individual furnace-wall layers are temperature dependant. Therefore, Eq. (9) is solved iteratively.

$$q_{\mathrm{cond\,w}} = \frac{1}{\sum_{k=1}^{K}\left(\frac{d_k}{\lambda_k(T_k)}\right) + \frac{1}{a_{\mathrm{air}}}}(T_{\mathrm{w}} - T_{\mathrm{air}}) \tag{9}$$

The total heat flux $q_{\mathrm{total},j}$ on the billet surface element j is then calculated using Eq. (10):

$$q_{\mathrm{total},j} = q_{\mathrm{rad\,gb}}(T_{\mathrm{g}}, T_{\mathrm{b}}) + q_{\mathrm{conv\,gb}}(T_{\mathrm{g}}, T_{\mathrm{b}}) + q_{\mathrm{rad\,wb},j} - q_{\mathrm{abs\,g}}(T_{\mathrm{g}}) \tag{10}$$

The calculation of $q_{\mathrm{rad\,gb}}(T_{\mathrm{g}}, T_{\mathrm{b}})$ in (10) is analogous to that for $q_{\mathrm{rad\,gw}}(T_{\mathrm{g}}, T_{\mathrm{w}})$ by (5):

$$q_{\mathrm{rad\,gb}}(T_{\mathrm{g}}, T_{\mathrm{b}}) = \varepsilon_{\mathrm{g}}(T_{\mathrm{g}})\sigma T_{\mathrm{g}}^4 - \alpha_{\mathrm{g}}(T_{\mathrm{g}}, T_{\mathrm{b}})\sigma T_{\mathrm{b}}^4 \tag{11}$$

The calculation of $q_{\mathrm{conv\,gb}}(T_{\mathrm{g}}, T_{\mathrm{b}})$ in (10) is analogous to that for $q_{\mathrm{conv\,gw}}(T_{\mathrm{g}}, T_{\mathrm{w}})$ using (6):

$$q_{\mathrm{conv\,gb}}(T_{\mathrm{g}}, T_{\mathrm{b}}) = a_{\mathrm{gb}} \cdot (T_{\mathrm{g}} - T_{\mathrm{b}}) \tag{12}$$

For an exact geometrical treatment in the model, the radiation heat exchange $q_{\mathrm{rad\,wb},j}$ in Eq. (10) is calculated as the difference between the incoming $q_{j\leftarrow}$ and the outgoing $q_{j\rightarrow}$ thermal radiation to the billet surface element j (13):

$$q_{\mathrm{rad\,wb},j} = q_{j\leftarrow} - q_{j\rightarrow} = \sum_{i=1}^{I} \varepsilon_i(T_i)\sigma T_i^4 \frac{A_i}{A_j} F_{i\rightarrow j} - \varepsilon_j(T_j)\sigma T_j^4 \tag{13}$$

In Eq. (13), the incoming thermal radiation consists of the thermal radiation contributions of the individual surface elements described by the elements $F_{i\rightarrow j}$ of the view-factor matrix $\mathbf{F}$. The matrix $\mathbf{F}$ is calculated prior to the simulation for the whole furnace geometry, consisting of I surfaces.

When the total heat fluxes to all the billet surface elements are determined, the 3D heat conduction inside the billet is calculated using the finite-difference method.

3.2. The temperature of the furnace floor

The billets in the walking-beam furnace lie on the furnace floor. The spaces between the billets and the billet dimensions can be varied. The furnace floor is heated from other surfaces in furnace enclosure; these surfaces can be the furnace walls or the billet surfaces. When the space between the billets becomes smaller, the furnace floor becomes colder, because the floor area covered by the billets becomes larger. In order to determine the furnace-floor temperature a special procedure has been developed.

The length of the furnace floor is divided into M floor-surface elements, to fulfill the isothermal condition. For each floor-surface element n, the heat-flux balance equation is derived (Fig. 3(b)):

$$q_{n\leftarrow} - q_{n\rightarrow} - q_{\mathrm{cond\,floor},n} = 0 \tag{14}$$

The incoming heat flux $q_{n\leftarrow}$ can be determined as the sum of the contributions of the surfaces in the furnace enclosure (15), by considering the elements $F_{m\to n}$ of the view-factor matrix **F**.

$$q_{n\leftarrow} = \sum_{m=1}^{M} \varepsilon_m(T_m)\sigma T_m^4 \frac{A_m}{A_n}\frac{N_{m\to n}}{N_m} = \sum_{m=1}^{M} \varepsilon_m(T_m)\sigma T_m^4 \frac{A_m}{A_n} F_{m\to n} \tag{15}$$

The outgoing heat flux $q_{n\to}$ in Eq. (14) due to thermal radiation can be calculated using Eq. (16). The temperature T_n is unknown. Therefore, the outgoing thermal flux cannot be determined directly.

$$q_{n\to} = \varepsilon_n(T_n)\sigma T_n^4 \tag{16}$$

The heat conduction through the furnace-floor element $q_{\text{cond floor},n}$ is evaluated using Eq. (9) by taking account of the material properties of the furnace-floor layers.

The calculation of all three thermal fluxes in Eq. (14) depends on the unknown temperature T_n of the furnace-wall element. The bisection method is used in the model to solve the balance Eq. (14) numerically, which gives the temperature of the furnace-floor element T_n.

3.3. Validation of the simulation model

The validation of the simulation model is a very important phase in the process of developing the simulation model. The model was validated on the basis of measurements on the OFU furnace in the Inexa Štore Steelworks in Slovenia.

The measurements were performed using five trailing thermocouples (Type K, $\phi = 5\,\text{mm}$, $L = 35\,\text{m}$). These five thermocouples were mounted on a test billet (Figs. 4 and 5). The temperatures were measured during the reheating of the billet as it passed through the furnace. The tuning of the model was performed simply by adjusting the temperature profile of the furnace's ceiling and sidewalls. After the tuning of the model, all the parameters of the model were within real

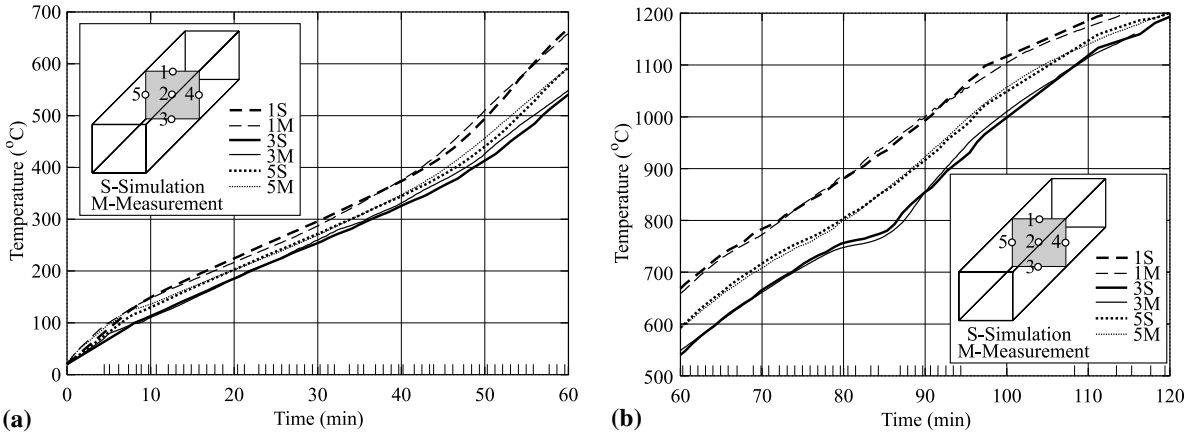

Fig. 4. Validation of the simulation model: a comparison between the simulation and the measurement results for measuring points 1, 3 and 5. The small vertical lines at the bottom of the graphs show the furnace steps during the measurements: (a) 0–60 min of reheating, (b) 60–120 min of reheating.

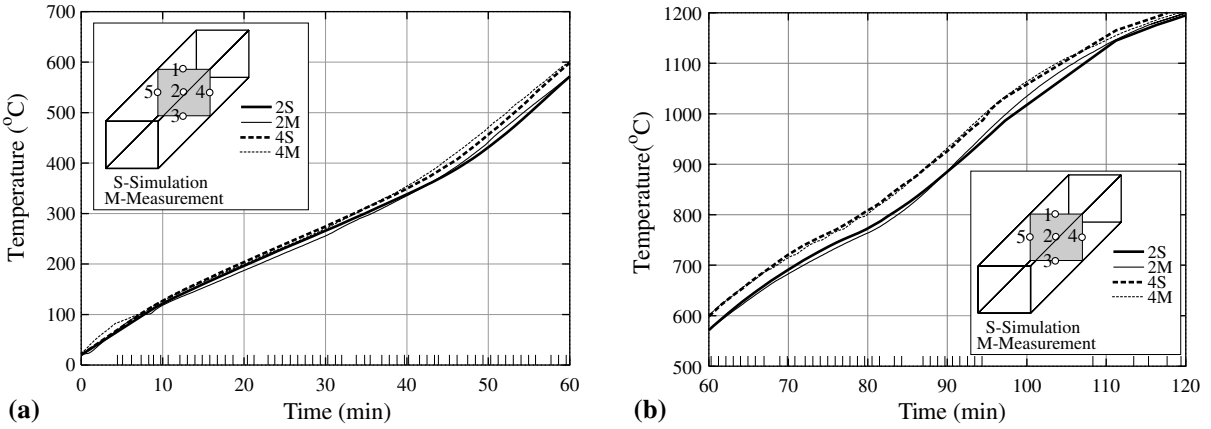

Fig. 5. Validation of the simulation model: a comparison between the simulation and the measurement results for measuring points 2 and 4. The small vertical lines at the bottom of the graphs show the furnace steps during the measurements: (a) 0–60 min of reheating, (b) 60–120 min of reheating.

physical values. Good agreement was obtained between the measured and the calculated temperatures at all five measuring points for the 120 min of the billet-reheating process (Figs. 4 and 5). The good agreement of the bottom-surface temperatures confirms that the algorithm for the furnace-floor temperature calculation is appropriate. The model takes into account the material properties of the reheated billets. The test billet of CK-45 Steel has a magnetic transformation at about 750 °C (a change in the specific heat at this temperature). This transformation can be seen in Fig. 4(b), measuring point 3 (solid lines), where the rise in the temperature of the bottom surface slows at around 750 °C. This phenomenon is observed in both the simulation and the measurement results.

The validation phase shows that the developed algorithms of the simulation model for billet reheating are in good agreement with the real physical behaviour of the reheating process.

4. Results

The simulations were performed for three billet sizes: (180 mm × 180 mm × 3500 mm), (220 mm × 220 mm × 3500 mm) and (300 mm × 300 mm × 3500 mm). The first two (180 mm and 220 mm) billet sizes were reheated during the normal production process; the third size (300 mm) was chosen to confirm the dependence for other billet sizes. The same criterion for discharging the billet from the furnace was used for all three sizes. The criterion is that the billet temperature in the centre should be at least 1235 °C, and the temperature difference between the upper and lower surfaces of the billet should be less than 10 °C.

The furnace productivity was simulated for different spaces between the billets. The graphs of furnace productivity for different billet dimensions, depending on the space between the billets, are shown in Figs. 6(a), (b) and 7(a). For each simulated space (each point in the graphs) the view-factor matrix **F** of the whole furnace was determined using the simulation model for the view-factor calculation. Next, the matrix **F** was used in the simulation model of the billet-reheating

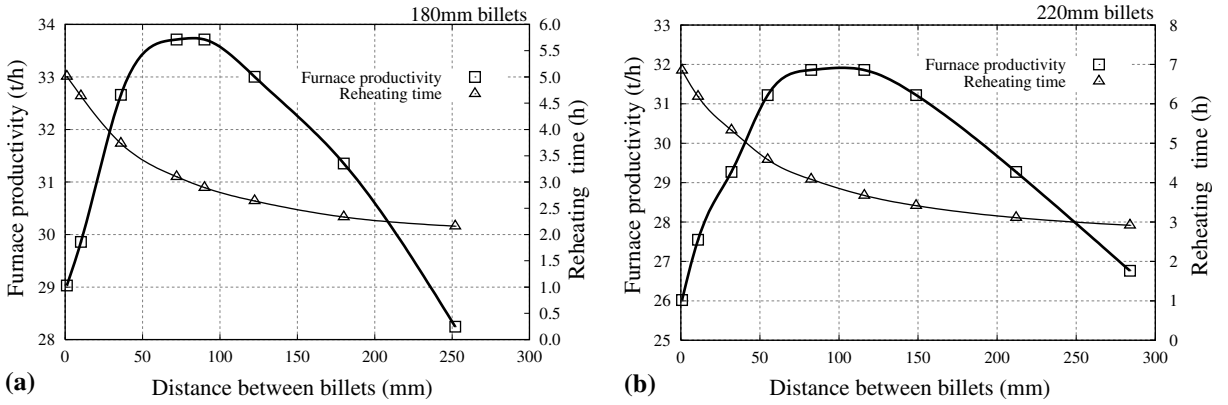

Fig. 6. Furnace productivity vs. the space between the billets for: (a) 180 mm billets and (b) 220 mm billets.

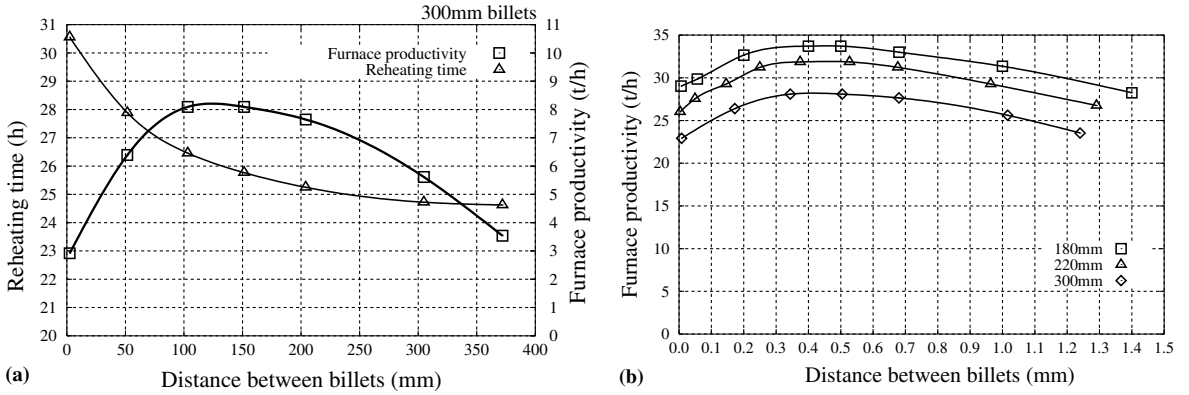

Fig. 7. (a) Furnace productivity vs. the space between the billets for 300 mm billets; (b) furnace productivity vs. normalized space between the billets.

process. The simulations of the billet reheating were performed many times for different time intervals between the furnace steps until the discharging criterion was satisfied.

It is clear from the graphs in Figs. 6(a), (b) and 7(a) that the productivity is very dependent on the space between the billets for all three sizes of billet. All three graphs show that an optimum space between billets exists, where the maximum productivity will be achieved.

For reheating conditions where there is no space between the billets, the long reheating times are significant (it takes approximately 5 h for a 180 mm billet, 7 h for a 220 mm billet and 10 h for a 300 mm billet). The main reason for the slow heating of the billet is the small area of heat exchange with the furnace (just the upper surface) and the low temperature of the furnace floor (because it is heated indirectly through the billet).

When the space between the billets becomes longer the productivity increases until the optimum space between billets is reached, where the maximum productivity is achieved. From Figs. 6(a), (b) and 7(a) it is clear that for the 180 mm billet the maximum productivity of 33.7 t/h is achieved with 80 mm of space between the billets; for the 220 mm billet the maximum productivity of 31.9 t/h is

achieved with 100 mm of space between the billets; and for the 300 mm billet the maximum productivity of 28.2 t/h is achieved with 120 mm of space between the billets.

When the space between the billets exceeds the optimum, the productivity is observed to decrease. Longer spaces between the billets give the billet a better geometrical position for intercepting the heat flux from the furnace with side surfaces and, as a result, the furnace floor becomes warmer. Therefore, the billets need a shorter reheating time, as can be seen in Figs. 6(a), (b) and 7(a). The reason why the productivity falls lies in its definition together with the nature of the continuous walking-beam furnace. When the billets are of the same size, the productivity is determined by the frequency of the furnace steps. In the continuous walking-beam furnace, the space between the billets determines the length of the furnace step. As a result, longer furnace steps, at the same frequency, give a shorter reheating time for the billets. When the space between the billets becomes longer than optimum, the reheating time becomes shorter, and does not allow the billet to reheat under the prescribed conditions. Therefore, the frequency of the furnace steps has to be reduced to satisfy the prescribed reheating conditions, which lowers the furnace productivity.

The comparison of furnace productivities for all three sizes of billet, depending on the normalized space between the billets, is presented in Fig. 7(b). The normalized space between the billets is, for a square cross-section, defined as:

$$\text{Normalized space between billets} = \text{space between billets}/\text{cross-sectional size}$$

The cross-sectional size represents the width or the height of the square-billet cross-section. In the cases investigated here the values of the cross-sectional size are 180 mm, 220 mm or 300 mm. The normalized space between the billets is a non-dimensional value. The comparison of the productivity curves in Fig. 7(b) shows that the highest productivity occurs for approximately the same normalized space between the billets for all three billet sizes, i.e., about 0.5. The highest productivity can be achieved when the space between the billets is half of the billet's cross-sectional size. This is also in agreement with Schuppe [8], who suggested the optimum space was between 0.3 and 0.7, based on measurements and observations.

5. Conclusion

The developed simulation model of the billet-reheating process considers the exact geometry in thermal radiation calculations of the furnace enclosure, including the geometry of the billets inside the furnace. The predictions of the developed simulation model for the billet-reheating process are in good agreement with the experimental data obtained from trailing thermocouples in real industrial furnace. The model was used for studying the productivity of a continuous walking-beam furnace for different spaces between billets, for three different sizes of billet. We found that the space between the billets has a significant effect on furnace productivity. The shape of the furnace-productivity curves shows that an optimum space exists, where the maximum productivity of the furnace can be achieved. When the space between the billets is normalized with the size of the billet's cross-section, the results show that the highest productivity is achieved for the same normalized space for all three simulated billet sizes. The value of the optimum normalized space is

about 0.5. This is also in agreement with Schuppe [8], who suggested the optimum space was between 0.3 and 0.7, based on measurements and observations.

References

[1] M.G. Carvalho, Mathematical Modelling of Industrial Furnaces and Boilers, Third European Conference on Industrial Furnaces and Boilers, INFUB, Rio Tinto, 1995, pp. 1–45.
[2] Computational Science Education Project, Monte Carlo Surface to Surface Particle Transport, 1995, www.csep1.phy.ornl.gov/pt/pt.html.
[3] W. Heiligenstaedt, Waermetechnische Rechnungen fuer Industrieoefen, Verlag Stahleisen M.B.H, Duesseldorf, 1966.
[4] A. Jaklič, B. Glogovac, T. Kolenko, B. Zupančič, B. Težak, A simulation of heat transfer during billet transport, Applied Thermal Engineering 22 (2002) 873–883.
[5] M. Matsumoto, T. Nisihimura, Twister Mersenne, A 632-dimensionally equidistributed uniform pseudorandom number generator, ACM transactions on modelling and computer simulations, Special Issue on Uniform Random Generation 8 (1) (1998) 3–30.
[6] M.F. Modest, Radiative Heat Transfer, McGraw-Hill Book Company, New York, 1993.
[7] R. Siegel, J.R. Howell, Thermal Radiation Heat Transfer, McGraw-Hill Book Company, New York, 1981.
[8] W. Schuppe, Erfahrungen mit Processrechnerfuehrungen an verschiedenen Ofentypen und Waermgutgeometrien, Stahl und Eisen 112 (8) (1992) 47–52.